fibers

MDPI

Article

Liquid Crystal Coated Yarns for Thermo-Responsive Textile Structures

Deña Mae Agra-Kooijman [1,*], Md Mostafa [1,2], Mourad Krifa [1,3,*], Linda Ohrn-McDaniel [3], John L. West [1,2] and Antal Jákli [1,2,4]

[1] Materials Science Graduate Program, Kent State University, Kent, OH 44242, USA
[2] Advanced Materials and Liquid Crystal Institute, Kent State University, Kent, OH 44242, USA
[3] School of Fashion Design and Merchandising, Kent State University, Kent, OH 44242, USA
[4] Department of Physics, Kent State University, Kent, OH 44242, USA
* Correspondence: dagrako@kent.edu (D.M.A.-K.); mkrifa@kent.edu (M.K.)

Abstract: We have developed a prototype of breathable thermochromic textile ideal for sensor applications, e.g., medical thermography. The textile was woven/knitted from polyester filaments pre-coated with thermochromic liquid crystal (TLC) ink, in lieu of coating the TLC ink on the woven/knitted textile. This process brings us closer to achieving breathable thermochromic textiles while enhancing the versatility of the textile. A combination of precoated yarns can be preselected according to the desired thermochromic properties of the textile. Swatches from both knitted and handwoven fabrics showed excellent reversible thermochromic property showing color from red to blue as the temperature is raised from 26 to 32 °C, consistent with the unincorporated TLC ink.

Keywords: liquid crystals; thermotropic textile; wearable fabric

check for updates

Citation: Agra-Kooijman, D.M.; Mostafa, M.; Krifa, M.; Ohrn-McDaniel, L.; West, J.L.; Jákli, A. Liquid Crystal Coated Yarns for Thermo-Responsive Textile Structures. *Fibers* **2023**, *11*, 3. https://doi.org/10.3390/fib11010003

Academic Editor: Catalin R. Picu

Received: 2 December 2022
Revised: 16 December 2022
Accepted: 20 December 2022
Published: 24 December 2022

Copyright: © 2022 by the authors. Licensee MDPI, Basel, Switzerland. This article is an open access article distributed under the terms and conditions of the Creative Commons Attribution (CC BY) license (https://creativecommons.org/licenses/by/4.0/).

1. Introduction

Throughout history, textile structures have served as interfaces between the human body and its environment with basic functions that include protection from the elements and aesthetic adornment. Rapid developments in material and processing technology in recent decades have led to a dramatic expansion of those functions. Today, textiles have transcended the role of adornment and passive protection to become interactive structures that integrate capabilities such as sensing and responding to stimuli from the environment. The resulting structures, dubbed smart textiles, can respond to stimuli of varied natures, including chemical, thermal, magnetic, and electrical [1–4].

Novel applications capitalizing on the capabilities of such smart textiles range from active protective clothing for frontline emergency response and military personnel [5,6], to environmentally responsive textiles that improve the quality of life and safety of consumers [6–8]. Another area of application of particular interest is biomedical textiles that detect and help diagnose health problems, [9–12] prevent infection and improve healing [13–15].

Recently, liquid crystals have emerged as suitable responsive sensing materials that can be incorporated into fibers and other textile structures [16–18]. Liquid crystals, discovered over 120 years ago, are a fascinating phase of matter that combine the order found in crystalline solids with the ability to flow like conventional liquids; thus, their name. Because of this combination of properties, liquid crystals are highly sensitive and responsive to external stimuli [16,19]. For instance, liquid crystals exhibit variations in optical properties when subjected to electrical fields. This property has led to them being the basis for the liquid crystal displays, LCDs, used in flat screen TVs and smartphone displays. In addition to displays, certain liquid crystals are thermochromic, changing color with changes in temperature, making them useful for thermometers and related sensors. More

recently liquid crystals have been shown to be very sensitive sensors for chemical environmental pollutants [20,21] as well as biomolecules and microorganisms such as bacteria and viruses [22,23].

As a practical matter, liquid crystals are often dispersed in polymer solutions to allow processing into various structures. Polymer dispersed liquid crystals, or PDLCs, were developed nearly 40 years ago. PDLCs encase the liquid crystal as microdomains in a polymer binder. Traditionally, the PDLCs have been made as solid films sandwiched between either glass or plastic substrates with transparent electrodes and are switched between scattering and transparent states upon application of an electric field. In addition to providing a mechanical encasement, polymers have also been used to stabilize liquid crystal structures in flat film forms as a means of enhancing their responsive properties.

Attempts have been made to incorporate liquid crystals into fibrous structures using various approaches. For instance, LCs have been dispersed into polymer solutions then electrospun into nano- and micro-fiber mats using single [20,24–26] or coaxial nozzles [27–29]. A new approach to form fibrous structures containing LCs was achieved through airbrushing of PDLC solutions [18,30]. It was found that airbrushing (or solution blow spinning) of a homogeneous polymer solution of low-molecular-weight LCs yields, through a phase separation process, uniform polymer fibers with a fluid liquid crystal core [18,30]. The solution blow spinning process was developed using polyvinylpyrrolidone (PVP) as the polymer sheath and resulted in mean fiber diameters ranging from approximately 1 μm to 3 μm depending on polymer concentration in the spinning solution.

Fiber diameters in the micron and submicron ranges have been common in published attempts to incorporate LCs into fibrous structures using the approaches discussed above. While such structures have great potential for thin-layer coating or laminate applications, the microscopic scale tends to limit the optical response to external stimuli of the LC core. Therefore, recent efforts by our team have sought to incorporate the responsive functionalities of LCs into larger-scale textile structures in conventional yarn and fabric forms. A recent development emanating from this effort yielded a simple laboratory procedure for coating staple and filament yarns with thermochromic cholesteric liquid crystals (CLCs) stabilized by an outer polymer sheath or by dispersing the liquid crystal in the coating polymer [19].

In this paper, we demonstrate the effectiveness of the coating process in imbuing textile yarns and fabrics with the ability of LC to respond to external stimuli. In addition, we explore further processing of the coated yarns into knit and woven fabrics and discuss qualitative and quantitative measures of the resulting fabric optical properties enabled by the LCs.

2. Materials and Methods

2.1. Materials

Two commercial thermochromic liquid crystals (SFXC and Hallcrest) were used. SFXC liquid crystal was purchased from Special FX Creative (East Sussex, UK) and used as received. That is, no further purification or dilution were made on the LC solution. The SFXC LC solution is a sprayable ink which changes color from red to green, and green to blue within a range of 5 °C [31]. The color red appears at 24 °C and blue at 29 °C. The second LC used is an aqueous, acrylic-based ink developed by Hallcrest LC (Series SPN300R24C3W) with a color band width of 3 °C with color red appearing at 24 °C and blue at 26 °C [32].

Initial feasibility tests to coat the LC thermochromic inks were conducted on a range of staple and multi-filament yarns. The yarn finally selected for fabric processing consisted of a black 100% polyester multifilament yarn (Repreve) with a linear density of 150 den/68 filaments. Black color was chosen for optimal color contrast.

2.2. Coating Process

Coating of the LC inks was done using the schematic in Figure 1. The bare yarn (Figure 1a-A) is looped through a series of pulleys and LC ink barrels (Figure 1a-B) then collected in the collector spool. Coating speed was controlled by a motor attached to the collector spool (Figure 1a-C) at 1 mm/s. Drying time of both inks is approximately 45 min at 20 °C. To avoid wet coat rolling into the pulleys, drying was accelerated by gently blowing warm air onto the coating before reaching the pulley, coupled with slow coating speed. The color brightness of the coats can be tailored by increasing the number of ink barrels. No polymer coat was necessary to stabilize the LC, thereby, no curing was done. Based on measurements averaged on five pieces of 3-feet long yarn, the weight of the coated yarn was 2.2 times that of the uncoated yarn.

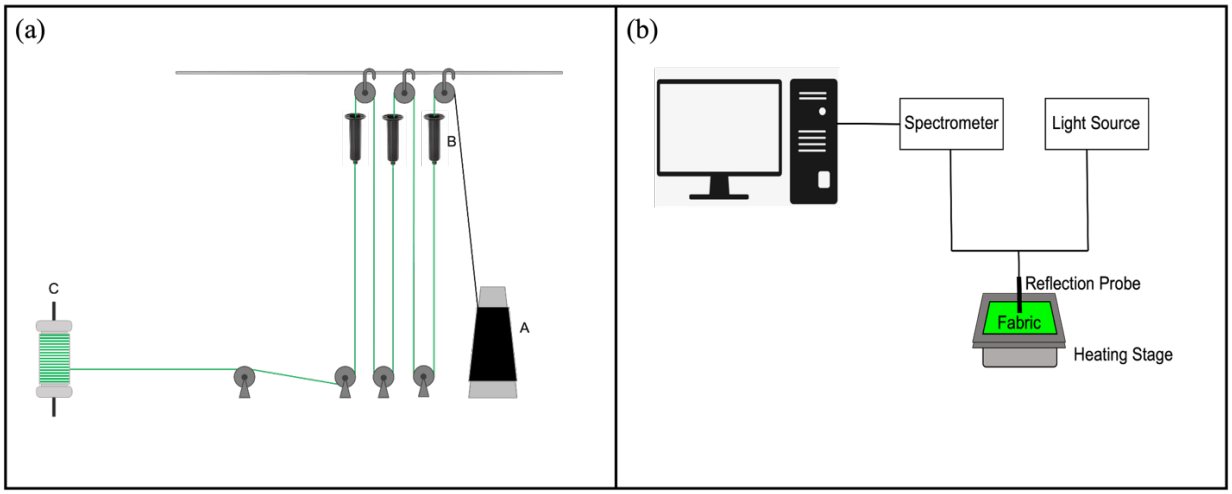


Figure 1. Schematics of (**a**) Yarn Coating Apparatus and (**b**) Reflectance Measurements. In (**a**), the bare yarn (A) is looped through pulleys and ink barrels (B), then dried before it is collected in the motorized spool (C). The measurements in (**b**) were made using a fiberoptic-based UV-VIS spectrometer consisting of reflection probe, light source and detector. Data was taken at various temperatures controlled by placing the fabric on a heating stage.

2.3. Fabric Construction: Weaving & Knitting

The coated yarns were hand woven, and machine knitted into swatches of thermochromic fabric to determine whether the ink can withstand shedding from both processes. The fabric swatches were then characterized to determine the temperature response of the fabric by measuring the reflectance at various temperatures. Bare polyester yarn was also machine knitted then painted with TLC ink for control measurements and comparisons.

An in-house weaving loom (Supplementary Information, SI Figure S1a) of width 3.5 inches was used to weave fabric swatch from black 100% polyester thread as warp and the LC-coated yarn as weft or the filling yarn. The focus is on characterizing the coated weft yarn component and therefore the uncoated warp thread count was minimized. Thus, the woven fabric was a plain weave with a thread count of 139 (11 warps and 128 wefts per inch) and resulting mass per unit area of 351 g/m^2.

Initial machine knitting experiments were conducted using a 7-gauge hand flat knitting machine to ensure the yarn could be processed with no visible shedding of the coating. Following successful hand flat knitting, the yarn was knitted on a 14-gauge flatbed digital knitting machine (Stoll CMS ADF-3, Figure S1b). The yarn was processed as 2 ends (for a resulting 2-ply denier of 2/150/68). Thus, a single jersey knitted fabric was produced with a needle point (NP) 11 and a corresponding 18 wales per inch (WPI) and 28 courses per inch (CPI).

2.4. Characterization

Longitudinal and cross-sectional micrographs of the coated yarn were obtained using field emission FEG Quanta 450 Scanning Electron Microscope (SEM) at 10 kV. In addition to yarn morphology, the yarn linear density and coating wt% add-on was measured according to ASTM D1907.

Fabric structure characteristics (Table 1) were measured based on current industry standards, including ASTM D3776/3776M (ASTM, 2009b) for mass per unit area (GSM), BS 5441:1988 (British Standards Institution, 1998) for knit fabric courses/inch and wales/inch counts, and ASTM D3775 for woven fabric end and pick counts [33].

Table 1. Fabric specifications and corresponding standards methods.

Fabric Property	Value	Standard Method
Plain weave, 100% polyester		
Mass per unit area (GSM)	351	ASTM D3776
End (warp) count/inch	11	ASTM D3775
Pick (filling) count/inch	128	ASTM D3775
Single Jersey, 100% polyester (14-gauge digital knitting machine swatch)		
Mass per unit area (GSM)	342	ASTM D3776
Courses/inch (CPI)	28	ASTM BS5441
Wales/inch (WPI)	18	ASTM BS5441
Single Jersey, 100% polyester (7-gauge hand knitting machine swatch)		
Mass per unit area (GSM)	110	
Courses/inch (CPI)	14.5	
Wales/inch (WPI)	10.75	

The images of thermochromic fabric were taken using microscope digital camera (AmScope MU1803) with 18-megapixel resolution. Reflectance measurements were done using fiberoptic-based UV-VIS spectrometer (Ocean Optics USV 2000+, 200–850 nm range) with Halogen light source (Ocean Optics LS-1, 400–800 nm range) and reflection probe (Ocean Optics R200-7-UV-VIS, 300–1100 nm range). The spectrometer covers the 200–850 nm range. Knitted fabric swatch from bare polyester black multifilament yarn was used for background subtraction. The schematic of the setup is shown in Figure 1b. The fabric is mounted on a hot plate with controlled heating ($\pm 0.1^{\circ}$ accuracy) for easy scanning at different temperature settings. All spectra were collected after ~30 s stabilization. The distance between the sample surface and the probe was adjusted until maximum reflection is achieved for each sample.

3. Results and Discussion

Prior to characterization, the yarns coated with SFXC and Hallcrest LC materials were tested for their durability during the hand knitting process. This test was necessary to check the possibility of LC layer coat shedding during the process of abrasion during knitting. When shedding occurred, the yarn could not be fed into the knitting machine as it would be detrimental to the operation of the machine. Retention of the coat is also critical for the thermotropic response which means that the thermotropic properties will be compromised after shedding. The Hallcrest material showed shedding of coat (Supplementary Material, Figure S1). This resulted in a less vibrant color when subjected to temperature changes. Therefore, no further tests were made on Hallcrest TLC ink. On the other hand, there was no shedding observed at all for the SFXC coated yarn during the hand knitting. This made it possible to characterize the coating in a knitted fabric swatch. Although both TLC ink formulations are micro-encapsulated, the difference in their formulations such as the matrix or solvent in which the LCs are microencapsulated could attribute to the shedding of the final coat. The TLC ink information from both Hallcrest and SFXC however are proprietary, therefore no comparison can be made. It can also be inferred that the SFXC

coating are embedded, not only on the surface of the multifilament yarn but also in between the filaments. This was verified from the morphology of the coated yarn using the SEM images.

3.1. Coated Yarn Morphology

The morphologies of the coated and uncoated yarns are shown in Figure 2.

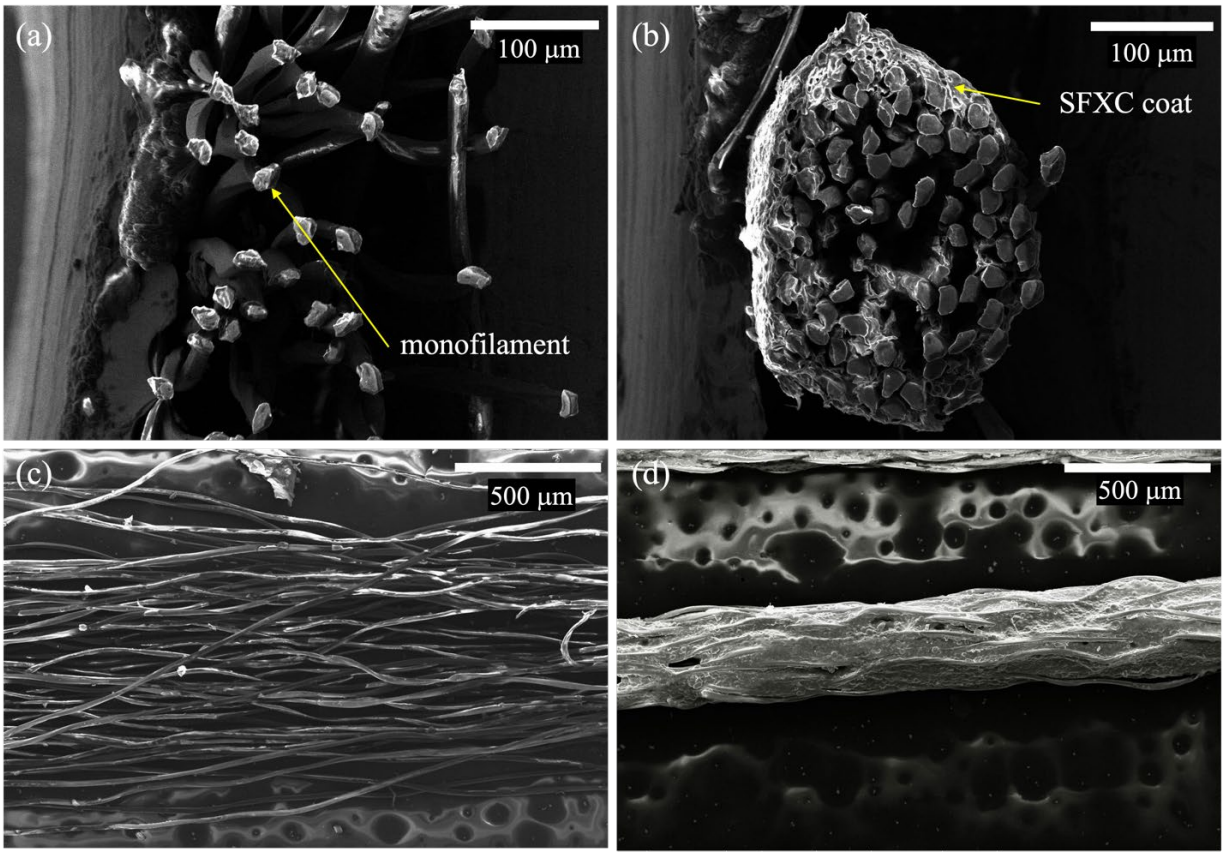


Figure 2. SEM images of multifilament Repreve yarn. Cross-section of the (**a**) splayed filaments of the uncoated yarn and (**b**) coated with SFXC liquid crystal. Longitudinal (side-on) images of the (**c**) uncoated and (**d**) coated yarn.

The uncoated yarn (Figure 2a) consisted of multifilament with average diameter size of 20.08 ± 2.30 µm (Supplementary Material, Figure S2). Figure 2c further reveals that the yarn was made-up of loose conglomerate of the filaments (untwisted). The coated yarn in Figure 2b has a slightly elliptic shape with diameters ~340 µm (major axis) and ~230 µm (minor axis). These lengths are much smaller than of the loose uncoated yarn diameter showing that the coating process compacted the monofilaments of the uncoated yarn. The coat is concentrated at the surface of the yarn which is contrary to the expectation that LCs are interspersed between the filaments. The coat surface is relatively smooth and has undulated structures (Figure 2d) which is most likely caused by the LC microcapsules (of size 13.4 ± 2.3 µm) that were uniformly embedded on the surface. The size distribution of the undulated structures is presented in Supplementary Material, Figure S3. It appears that SFXC TLC ink has excellent adhesion properties on the polyester filaments compared with the Hallcrest one.

3.2. Fabric Characteristics

To determine the color fastness of the thermotropic yarn against weaving and knitting processes, fabric swatches were made as described above. The fabric physical properties measured using those procedures are summarized in Table 1. The woven fabric swatch

size was 3.125 × 3.5 inches. The number of warps was counted across the width, while the pick yarn was counted randomly across the length per inch in different space of the swatch. The knitted jersey (circular swatch) had vertical gauge of 28 CPI and horizontal gauge of 18 WPI. The hand knitted swatch had a vertical gauge of 14.5 CPI and horizontal gauge of 10.75 WPI.

3.3. Thermochromic Response

Before weaving and knitting, the thermotropic characteristics of both TLC inks were qualitatively evaluated on the coated yarns wound in the bobbin by simply placing the fingers on the bobbin. Qualitative tests of thermochroic response on both the SFXC and Hallcrest LCs coats are shown before hands were placed on the spool (Figure 3a), during (Figure 3b) and after the hands were removed (Figure 3c–f). In Figure 3b, the Hallcrest LC coated yarn was more responsive as seen by the green color near the edge of the fingers on the spool (right side of Figure 3b). This is partially related to the fact that the Hallcrest coated yarn was brighter at room temperature than the SFXC. To remove the ambiguity of temperature gradients between left and right hands, the two spools were switched (Supplementary Material, Figure S4). Similar results were observed. The thermochromic behavior was highlighted from the images in Figure 3c–f at t = 0, 1, 5 and 10 s. The color changed from blue to red on SFXC coated yarn within 10 s, whereas the Hallcrest spool stayed green at t ~ 10 s. Assuming that the temperature change is the same for both spools, this shows that the coated SFXC has faster response time than Hallcrest coat, with the consideration of the color band width of unincorporated Hallcrest (3 °C) and SFXC (5 °C) inks. In addition, SFXC has greater color density than the Hallcrest.

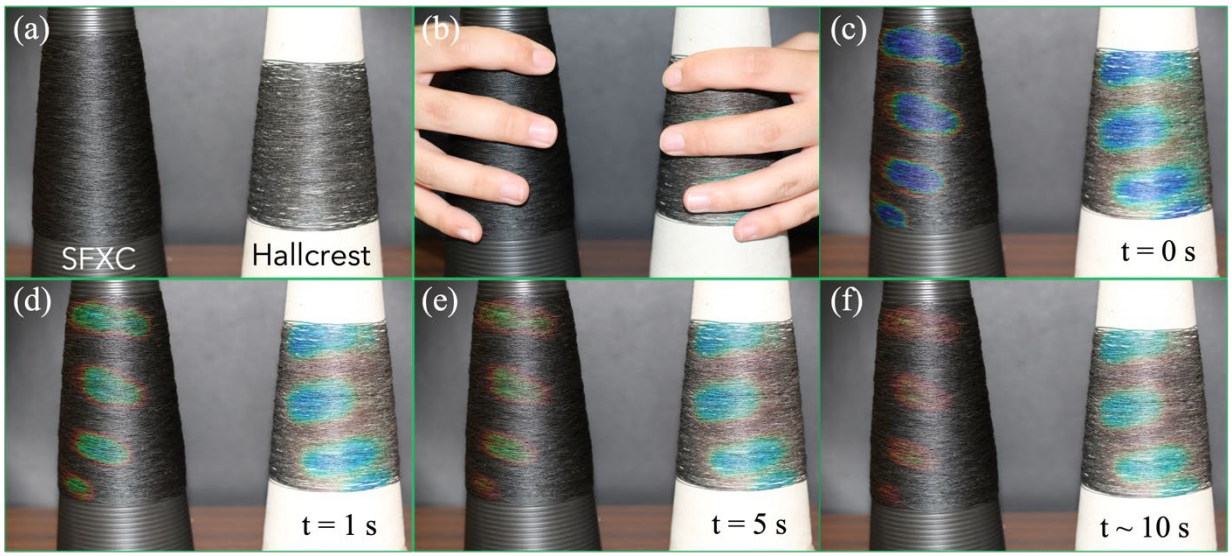


Figure 3. Spool of continuous SFXC and Hallcrest LC coated yarns showing the temperature response at different stages: (**a**) Before hands were placed on the spools. (**b**) Hands on the spools. (**c**) Immediately after the hands were removed (t = 0). Color play at (**d**) t = 1 s, (**e**) t = 5 s, and (**f**) t ~10 s.

After the weaving and knitting process the thermochromic properties are retained without significant decrease in the color density for SFXC coat. Figure 4 highlights the qualitative thermochromic behavior of woven (Figure 4a) and knitted (Figure 4b) swatches of SFXC coated polyester yarn at temperatures 27, 28 and 29 °C to show the red, green, and blue color shifts, respectively.

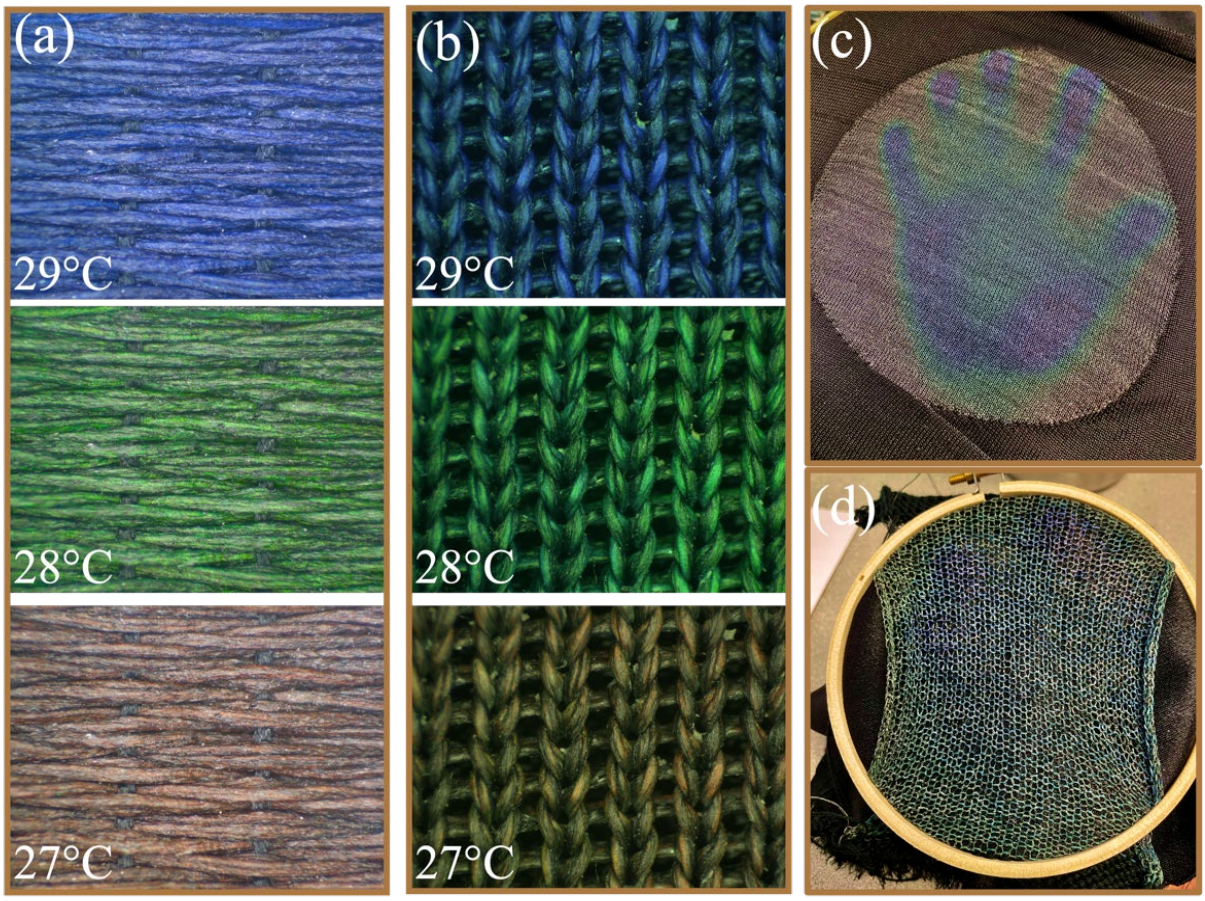


Figure 4. Images of hand woven (**a**) and knitted (**b**) fabrics of SFXC LC coated polyester yarns. (**c**) Machine knitted fabric with black satin fabric underlay revealing the hand placed underneath the fabric. (**d**) Handknitted fabric showing temperature inhomogeneity.

The color density of the SFXC coat was preserved during the knitting process as highlighted in Figure 4c which shows the machine knitted fabric (28 CPI, 18 WPI). As can be seen, the imprint was a result of the thermochromic response of the fabric upon contact with warm palm. Note that the boundaries between different temperature of the palm were well defined demonstrating that the textile made from SFXC coated yarn are appropriate for thermography across contoured surfaces with complex thermal features. The palm imprint however of the hand knitted fabric swatch (14.5 CPI, 10.75 WPI) was inhomogeneous across the fabric and barely recognizable. A black satin fabric underlay was placed under the knitted fabrics to maximize the color contrast. This is mainly attributed to the thread/yarn count which is much smaller for the hand knitted swatch. This demonstrated that accuracy of thermal mapping can be greatly improved by increasing the thread count of the textile made from these coated filaments. One can envision a composite textile for chronic wound thermography or incorporate a network of these coated filaments in bandages or diabetic socks. The TLC coat can be carefully selected and incorporated into woven or knitted fabrics as drapeable bandage suitable to the range of temperature for wound mapping, or specific part of the human body temperature mapping.

Color fastness to UV was tested by exposing the spool of coated yarn in direct sunlight for a month before knitting or weaving (Supplementary Material, Figure S5). The color density and thermochromic behavior were preserved after prolonged exposure to sunlight.

The tolerance to high humidity was not tested. However, a study on liquid crystal polymer composite fibers by Wang et al. [34] showed that the fibers were insensitive to humidity provided that both the LC and polymer were hydrophobic. This condition holds

in our system, therefore the same tolerance to high humidity is expected. Nevertheless, humidity tolerance test is considered for future study.

3.4. Reflectance

To quantify the color density (brilliance) of the thermochromic fabric swatches, their reflection spectra are shown in Figure 5a. The reflectance curves of SFXC coated yarn wound around glass slide and fabric swatches at 29 °C are shown in Figure 5a for comparison of their color density or brilliance.

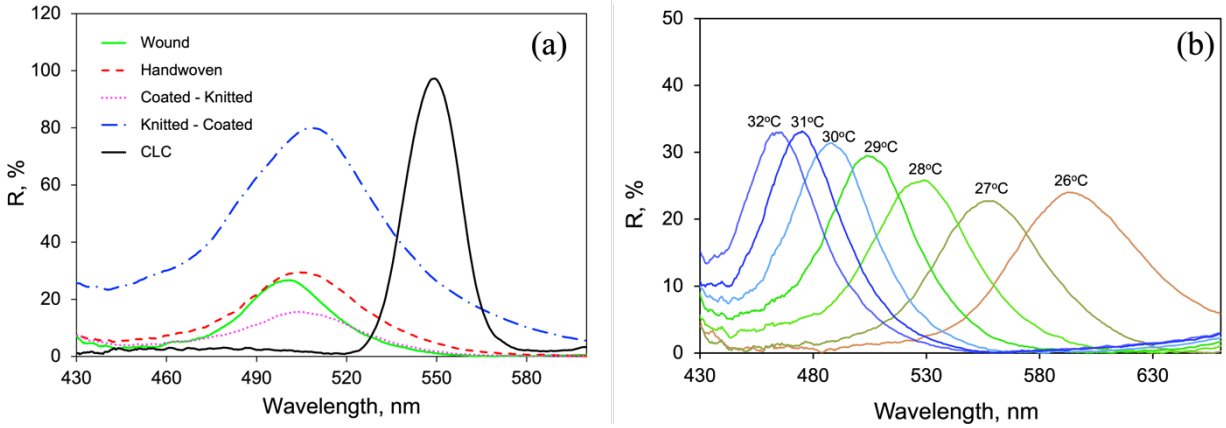


Figure 5. Reflectance of SFXC coated yarn and fabric. (**a**) Comparison of the reflectance of the yarn and fabric swatch with a regular cholesteric liquid crystal (CLC) sandwiched between two cover slips (black solid line), wound coated fibers around glass plate (green solid line), handwoven (red dashed line), knitted after coating process (magenta dotted line) and coated after knitting bare yarn (blue dash-dotted line). (**b**) Reflectance spectra showing the shift of λ_{max} with temperature.

The position of the maximum wavelength (λ_{max}) and peak values were determined from the fits to the spectra and recorded in Table 2. For comparison, the spectrum of pure cholesteric liquid crystal (CLC) sandwich between two glass cover slips was included in Figure 5a (black solid line) with maximum wavelength (λ_{max}) centered at ~550 nm and peak height of 96.95%. It is noted here that the magnitude of the reflectance values are absolute measurements and not relative to a white background (100%). As mentioned in Section 2.4, the distance between the probe and sample surface was adjusted to maximize the achievable reflection for all samples to compensate for the different fabric thicknesses. The high reflectance value was expected from CLC in this configuration with the cholesteric helix axis oriented perpendicular to the glass surface. The reflectance value of 71.2% at λ_{max} = 509 nm for the paint brush coated swatch of knitted bare yarn (Knitted-Coated in Figure 5a, blue dash-dot line) illustrate that high reflectance was achievable for SFXC ink and comparable to CLC. Notably, the painted coat on the knitted, bare-yarn fabric swatch was considerably thicker than the coat on the yarn. The broadening of the peak is due to the distribution of the orientation of helical axis of the liquid crystal within the microcapsule ink with respect to the fabric surface. The λ_{max} for hand woven (red dashed line) and knitted (magenta dotted line) fabric swatches were both centered at ~505 nm while λ_{max} for the wound yarn around the glass slide was shifted to 498 nm. This wavelength shift could be attributed to the small temperature gradients through the glass. The peak height for the wound coated yarn (26.0%) was comparable to that of the hand woven one (28.9) and demonstrates that the LC coat remains uncompromised after the weaving process. This was not the case for the knitted SFXC coated yarn with peak height of 13.8% which was less than the value of the uncoated one, a clear indication that the knitting is an abrasive process and compromised the integrity of the coating. Nevertheless, the thermotropic properties were maintained as highlighted in Figure 5b showing a temperature sweep (26–32 °C) of the reflection spectra. The maximum reflected wavelength (λ_{max}) shifted from the blue end of the visible spectrum at T = 32 °C to the red end of the spectrum at 26 °C with decreasing

temperature. Red color appeared at 26 °C, green at 27–29 °C and blue at 30–32 °C. This thermotropic behavior was completely reversible.

Table 2. Quantitative comparison of the color density of fabric swatches from peak values at λ_{max}.

Sample Configuration	λ_{max} (nm)	$R_{peak\ height}$ (%)
CLC	550	96.7
Knitted-Coated [1]	509	71.2
Hand Woven	506	28.9
Wound coated yarn around glass substrate	498	26.0
Coated-Knitted [2]	506	13.8

[1] Means that the bare yarn was first knitted then coated with TLC ink. [2] The yarn was coated first then knitted.

The color change from red to blue span across the temperature interval of 7 °C, which was 2 degrees wider than the SFXC in solution. This shift of the interval may be attributed to compositional and/or conformational changes of the microcapsules when embedded on the surface polyester yarn.

The nature of the coated yarn material provides versatility of application. For example, a network of hand-woven fabric from a combination of yarns coated with specific TLC inks with various temperature ranges can be made by appropriate selection of the TLC inks. In addition, the TLC coated yarn can also be knitted with photochromic or conductive yarns, expanding the range of application of the textile, and making smart textile smarter.

4. Conclusions

In this paper, we have demonstrated the effectiveness of imbuing textile yarns and fabric with the ability to respond to temperature by coating thermochromic LC inks. Specifically, this study showed that coating the yarn before the knitting or weaving was effective for some commercially available TLC inks despite the rigorous abrasive process. The process is ideal for applications that require breathable smart textile and versatile functions. Knitted/woven SFXC fabric swatches revealed excellent reversible thermochromic response from red to blue and vice versa within the range of 26–32 °C. Hallcrest coats underwent severe shedding compromising its thermochromic property and the color density. This study also led us to further explore and develop new TLC ink formulations with better color brilliance than commercially available ones and with outstanding stability against abrasive processes such as machine knitting and weaving [35]. Improvements in retaining the brilliance of the coat after knitting/weaving process is currently being explored.

Supplementary Materials: The following supporting information can be downloaded at: https://www.mdpi.com/article/10.3390/fib11010003/s1, Figure S1: (a) in-house weaving equipment. (b) Knitting machine.; Figure S2.: Filament size distribution.; Figure S3: Microcapsules Size Distribution of the SFXC coat.; Figure S4: Comparison of the color response between SFXC and Hallcrest when position of the bobbins was switched from left to right. Showed that the hands were of equal or comparable temperatures.

Author Contributions: Conceptualization, D.M.A.-K., J.L.W. and A.J.; methodology, D.M.A.-K., M.M., M.K., L.O.-M.; validation, D.M.A.-K. and M.M.; formal analysis, A.J., J.L.W. and D.M.A.-K.; investigation, M.K. and L.O.-M., resources; J.L.W., A.J., M.K. and L.O.-M.; data curation, D.M.A.-K. and M.M.; writing—original draft preparation, M.K. and D.M.A.-K.; writing—review and editing, A.J. and J.L.W.; supervision, A.J. and J.L.W.; funding acquisition, A.J. and J.L.W. All authors have read and agreed to the published version of the manuscript.

Funding: This work was carried out with the financial support by Kent State University and Cleveland State University Technology Validation and Start-Up Fund (KCTVSF).

Acknowledgments: The authors would like to thank Merrill Groom for making the coating setup.

Conflicts of Interest: The authors declare no conflict of interest.

References

1. van Langenhove, L. Smart textiles for protection: An overview. In *Smart Textiles for Protection*; Chapman, R.A., Ed.; Woodhead: Oxford, UK, 2013; pp. 3–33.
2. Koncar, V. Introduction to smart textiles and their applications. In *Smart Textiles and their Applications*; Koncar, V., Ed.; Woodhead: Oxford, UK, 2016; pp. 1–8.
3. Kongahage, D.; Foroughi, J. Actuator Materials: Review on Recent Advances and Future Outlook for Smart Textiles. *Fibers* **2019**, *7*, 21. [CrossRef]
4. Krifa, M. Electrically Conductive Textile Materials—Application in Flexible Sensors and Antennas. *Textiles* **2021**, *1*, 239–257. [CrossRef]
5. Laufer, G.; Kirkland, C.; Cain, A.A.; Grunlan, J.C. Clay–Chitosan Nanobrick Walls: Completely Renewable Gas Barrier and Flame-Retardant Nanocoatings. *ACS Appl. Mater. Interfaces* **2012**, *4*, 1643–1649. [CrossRef] [PubMed]
6. Bhuiyan, M.A.R.; Wang, L.; Ding, J.; Shaid, A.; Shanks, R.A. Advances and applications of chemical protective clothing system. *J. Ind. Text.* **2018**, *49*, 97–138. [CrossRef]
7. Shastri, J.P.; Rupani, M.G.; Jain, R.L. Antimicrobial activity of nanosilver-coated socks fabrics against foot pathogens. *J. Text. Inst.* **2012**, *103*, 1234–1243. [CrossRef]
8. Pakdel, E.; Naebe, M.; Sun, L.; Wang, X. Advanced Functional Fibrous Materials for Enhanced Thermoregulating Performance. *ACS Appl. Mater. Interfaces* **2019**, *11*, 13039–13057. [CrossRef]
9. Liu, L.; Jia, N.; Zhou, Q.; Yan, M. Electrochemically fabricated nanoelectrode ensembles for glucose biosensors. *Mater. Sci. Eng. C* **2007**, *27*, 57–60. [CrossRef]
10. Ekanayake, E.M.I.; Preethichandra, D.M.G.; Kaneto, K. Polypyrrole nanotube array sensor for enhanced adsorption of glucose oxidase in glucose biosensors. *Biosens. Bioelectron.* **2007**, *23*, 107–113. [CrossRef]
11. Nambiar, S.; Yeow, J.T.W. Conductive polymer-based sensors for biomedical applications. *Biosens. Bioelectron.* **2011**, *26*, 1825–1832. [CrossRef]
12. Gualandi, I.; Tessarolo, M.; Mariani, F.; Possanzini, L.; Scavetta, E.; Fraboni, B. Textile Chemical Sensors Based on Conductive Polymers for the Analysis of Sweat. *Polymers* **2021**, *13*, 894. [CrossRef]
13. Mirzaei, H.; Darroudi, M. Zinc oxide nanoparticles: Biological synthesis and biomedical applications. *Ceram Int.* **2017**, *43*, 907–914. [CrossRef]
14. Naseri, N.; Algan, C.; Jacobs, V.; John, M.; Oksman, K.; Mathew, A.P. Electrospun chitosan-based nanocomposite mats reinforced with chitin nanocrystals for wound dressing. *Carbohydr. Polym.* **2014**, *10*, 7–15. [CrossRef]
15. Ignatova, M.; Manolova, N.; Rashkov, I. Electrospun Antibacterial Chitosan-Based Fibers. *Macromol. Biosci.* **2013**, *13*, 860–872. [CrossRef]
16. Wang, J.; Jákli, A.; Guan, Y.; Fu, S.; West, J. Developing Liquid-Crystal Functionalized Fabrics for Wearable Sensors. *Soc. Inf. Disp.* **2017**, *33*, 16–20. [CrossRef]
17. Wang, J.; Kolacz, J.; Chen, Y.; Jákli, A.; Kawalec, J.; Benitez, M.; West, J.L. Smart Fabrics Functionalized by Liquid Crystals. *Soc. Inf. Disp. Symp. Dig. Tech. Pap.* **2017**, *48*, 147–149. [CrossRef]
18. West, J.L.; Wang, J.; Jákli, A. Airbrushed Liquid Crystal/Polymer Fibers for Responsive Textiles. *Adv. Sci. Technol.* **2016**, *100*, 43–49.
19. Guan, Y.; Agra-Kooijman, D.M.; Fu, S.; Jákli, A.; West, J.L. Responsive Liquid-Crystal-Clad Fibers for Advanced Textiles and Wearable Sensors. *Adv. Mater.* **2019**, *31*, 1902168. [CrossRef]
20. Agra-Kooijman, D.M.; Robb, C.; Guan, Y.; Jákli, A.; West, J.L. Liquid crystal core polymer fiber mat electronic gas sensors. *Liq. Cryst.* **2021**, *48*, 1880–1887. [CrossRef]
21. Lai, Y.T.; Kuo, J.C.; Yang, Y.J. A novel gas sensor using polymer-dispersed liquid crystal doped with carbon nanotubes. *Sens. Actuators A Phys.* **2014**, *215*, 83–88. [CrossRef]
22. Sivakumar, S.; Wark, K.L.; Gupta, J.K.; Abbott, N.L.; Caruso, F. Liquid Crystal Emulsions as the Basis of Biological Sensors for the Optical Detection of Bacteria and Viruses. *Adv. Funct. Mater.* **2009**, *19*, 2260–2265. [CrossRef]
23. Otón, E.; Otón, J.M.; Caño-García, M.; Escolano, J.M.; Quintana, X.; Geday, M.A. Rapid detection of pathogens using lyotropic liquid crystals. *Opt. Express.* **2019**, *27*, 10098–10107. [CrossRef] [PubMed]
24. Buyuktanir, E.A.; Frey, M.W.; West, J.L. Self-assembled, optically responsive nematic liquid crystal/polymer core-shell fibers: Formation and characterization. *Polymer* **2010**, *51*, 4823–4830. [CrossRef]
25. Buyuktanir, E.A.; West, J.L.; Frey, M.W. Optically responsive liquid crystal microfibers for display and nondisplay applications. In *Proceedings SPIE, Emerging Liquid Crystal Technologies*; SPIE: Bellingham, WA, USA, 2011.
26. Lagerwall, J.P.F.; Scalia, G. A new era for liquid crystal research: Applications of liquid crystals in soft matter nano-, bio- and microtechnology. *Curr. Appl. Phys.* **2012**, *12*, 1387–1412. [CrossRef]
27. Enz, E.; Lagerwall, J. Electrospun microfibres with temperature sensitive iridescence from encapsulated cholesteric liquid crystal. *J. Mater. Chem.* **2010**, *20*, 6866–6872. [CrossRef]
28. Reyes, C.G.; Sharma, A.; Lagerwall, J.P.F. Non-electronic gas sensors from electrospun mats of liquid crystal core fibres for detecting volatile organic compounds at room temperature. *Liq. Cryst.* **2016**, *43*, 1986–2001. [CrossRef]
29. Nguyen, J.; Stwodah, R.M.; Vasey, C.L.; Rabatin, B.E.; Atherton, B.; D'Angelo, P.A.; Swana, K.W.; Tang, C. Thermochromic Fibers via Electrospinning. *Polymers* **2020**, *12*, 842. [CrossRef]

30. Wang, J.; Jákli, A.; West, J.L. Airbrush Formation of Liquid Crystal/Polymer Fibers. *ChemPhysChem* **2015**, *16*, 1839–1841. [CrossRef]
31. Temperature Responsive Liquid Crystal Sprayable Ink. Available online: https://www.sfxc.co.uk/products/sfxc-sprayable-liquid-crystal-ink (accessed on 20 March 2019).
32. TLC Products for Use in Research and Testing Applications. Available online: https://www.lcrhallcrest.com/wp-content/uploads/2019/02/RD-TLC-Products-for-use-in-Research-Testing-Applications.pdf (accessed on 19 June 2020).
33. *ASTM D3775-18*; ASTM, Standard Test Method for End (Warp) and Pick (Filling) Count of Woven Fabrics. American Society for Testing and Materials: West Conshohocken, PA, USA, 2018.
34. Wang, J.; Jákli, A.; West, J.L. Liquid crystal/polymer fiber mats as sensitive chemical sensors. *J. Mol. Liq.* **2018**, *267*, 490–495. [CrossRef]
35. Mostafa, M.; Agra-Kooijman, D.M.; Perera, K.; Adaka, A.; West, J.L.; Jákli, A. Colloidal Latex/Liquid Crystal Coatings for Thermochromic Textiles. *Col. Interface Sci. Commun.* 2022, *under reviewing*.

Disclaimer/Publisher's Note: The statements, opinions and data contained in all publications are solely those of the individual author(s) and contributor(s) and not of MDPI and/or the editor(s). MDPI and/or the editor(s) disclaim responsibility for any injury to people or property resulting from any ideas, methods, instructions or products referred to in the content.